Predicting Two-Phase Pressure Drops in Vertical Pipe

J. ORKISZEWSKI*

ESSO PRODUCTION RESEARCH CO.
HOUSTON, TEX.

ABSTRACT

A method is presented which can accurately predict, with a precision of about 10 percent, two-phase pressure drops in flowing and gas-lift production wells over a wide range of well conditions. The method is an extension of the work done by Griffith and Wallis[11] and was found to be superior to five other published methods. The precision of the method was verified when its predicted values were compared against 148 measured pressure drops. The unique features of this method over most others are that liquid holdup is derived from observed physical phenomena, the pressure gradient is related to the geometrical distribution of the liquid and gas phase (flow regimes), and the method provides a good analogy of what happens inside the pipe. It takes less than a second to obtain a prediction on the IBM 7044 computer.

INTRODUCTION

The problem of accurately predicting pressure drops in flowing or gas-lift wells has given rise to many specialized solutions for limited conditions, but not to any generally accepted one for broad conditions. The reason for these many solutions is that the two-phase flow is complex and difficult to analyze even for the limited conditions studied. Under some conditions, the gas moves at a much higher velocity than the liquid. As a result, the down-hole flowing density of the gas-liquid mixture is greater than the corresponding density, corrected for down-hole temperature and pressure, that would be calculated from the produced gas-liquid ratio. Also, the liquid's velocity along the pipe wall can vary appreciably over a short distance and result in a variable friction loss. Under other conditions, the liquid is almost completely entrained in the gas and has very little effect on the wall friction loss. The difference in velocity and the geometry of the two phases strongly influence pressure drop. These factors provide the basis for categorizing two-phase flow. The generally accepted categories (flow regimes) of two-phase flow are bubble, slug, (slug-annular) transition and annular-mist.** They are ideally depicted in Fig. 1 and briefly described as follows.

BUBBLE FLOW (FIG. 1A)

The pipe is almost completely filled with the liquid and the free-gas phase is small. The gas is present as small bubbles, randomly distributed, whose diameters also vary randomly. The bubbles move at different velocities depending upon their respective diameters. The liquid moves up the pipe at a fairly uniform velocity and, except for its density, the gas phase has little effect on the pressure gradient.

SLUG FLOW (FIG. 1B)

In this regime, the gas phase is more pronounced. Although the liquid phase is still continuous, the gas bubbles coalesce and form stable bubbles of approximately the same size and shape which are nearly the diameter of the pipe. They are separated by slugs of liquid. The bubble velocity is greater than that of the liquid and can be predicted in relation to the velocity of the liquid slug.[12] There is a film of liquid around the gas bubble. The liquid velocity is not constant—whereas the liquid slug always moves upward (in the direction of bulk flow); the liquid in the film may move upward but possibly at a lower velocity, or it may move downward. These varying liquid velocities will result not only in varying wall friction losses, but also in a "liquid holdup" which will influence flowing density. At higher flow velocities, liquid can even be entrained in the gas bubbles. Both the gas and liquid phases have significant effects on the pressure gradient.

TRANSITION FLOW (FIG. 1C)

The change from a continuous liquid phase to a continuous gas phase occurs in this region. The liquid slug between the bubbles virtually disappears, and a significant amount of liquid becomes entrained in the gas phase. Although the effects of the liquid are significant, the gas phase is more predominant.

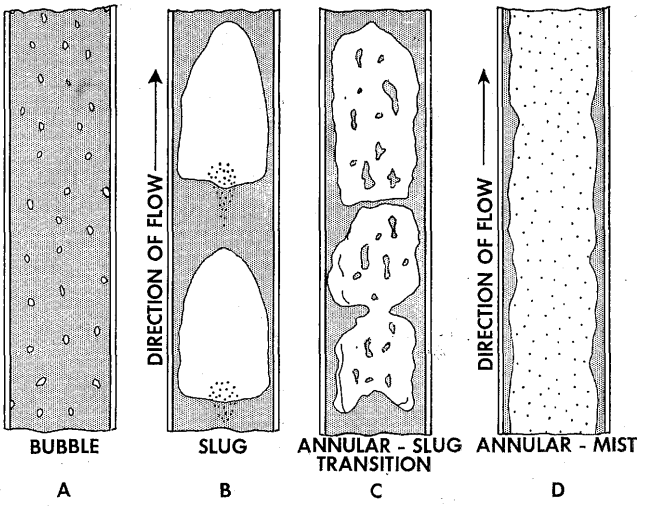

FIG. 1—GEOMETRICAL CONFIGURATIONS IN VERTICAL FLOW.

Original manuscript received in Society of Petroleum Engineers office August 8, 1966. Revised manuscript of SPE 1546 received March 1, 1967. Paper was presented at 41st Annual Fall Meeting held in Dallas, Tex., Oct. 2-5, 1966.

*Presently with International Petroleum Co. Ltd., Talara, Peru.

[11]References given at end of paper.

**All four regimes could conceivably exist in the same well. An example would be a deep well producing light oil from a reservoir which is near its bubble point. At the bottom of the hole, with little free gas present, flow would be in the bubble regime. As the fluid moves up the well, the other regimes would be encountered because gas continually comes out of solution, and the pressure continually decreases. Normally, however, flow is in the slug regime and rarely in mist, except for condensate reservoirs or steam-stimulated wells.

ANNULAR-MIST FLOW (FIG. 1D)

The gas phase is continuous. The bulk of the liquid is entrained and carried in the gas phase. A film of liquid wets the pipe wall, but its effects are secondary. The gas phase is the controlling factor.

To cope with the complex problem, the many published methods were analyzed to determine whether any one method was broad enough, or had the ingredients to be broad enough, to accurately predict pressure drops over a wide range of well conditions. The methods were first categorized. Certain methods were selected from each category to predict pressure drops for two selected well cases whose flow conditions were significantly different from those originally used in developing the various methods. Finally, the predicted pressure drops using the more promising methods were compared against known values taken from 148 cases having widely varying conditions of rate, GOR, tubing size, water cut and fluid properties.

BASIS FOR SELECTING METHODS STUDIED

Based upon similarity in theoretical concepts, the published methods were first divided into three categories. From each category certain methods were selected, based on whether they were original or unique, and were developed from a broad base of data. The discriminating features of the three categories are shown.

CATEGORY 1 (REFS. 1, 3-6, 9)

Liquid holdup is not considered in the computation of the density. The density is simply the composite density of the produced (top-hole) fluids corrected for down-hole temperature and pressure. The liquid holdup and the wall friction losses are expressed by means of an empirically correlated friction factor. No distinctions are made among flow regimes.

CATEGORY 2 (REFS. 7, 8, 10)

Liquid holdup is considered in the computation of the density. The liquid holdup is either correlated separately or combined in some form with the wall friction losses. The friction losses are based on the composite properties of the liquid and gas. No distinctions are made among flow regimes.

CATEGORY 3 (REFS. 2, 11-13)

The calculated density term considers liquid holdup. Liquid holdup is determined from some concept of slip velocity (the difference between the gas and liquid velocities). The wall friction losses are determined from the fluid properties of the continuous phase. Four distinct flow regimes are considered.

Of the 13 methods categorized, two from each category were selected for further study. The methods of Poettmann and Carpenter,[1] and Tek[4] were picked from Category 1. Most of the methods in this category are extensions of the Poettmann-Carpenter work. In the second category, the Hughmark and Pressburg method[8] was selected; the Hagedorn and Brown method[10] was not available at the time of the initial screening, but it was included in the final detailed evaluation. There are really only two methods in Category 3. The Griffith[12] and the Griffith and Wallis[11] methods are synonymous; the Nicklin, Wilkes, and Davidson method[13] is for special conditions and parallels the work of Griffith-Wallis. The other method is that of Duns and Ros.[2]

RESULTS OF THE COMPARISON

The five methods initially selected, whose results were hand calculated, were compared by determining the deviation between predicted and measured pressure drops for the first two well conditions listed in Table 1. Fig. 2 compares the predictions for Well 1. The results were similar for Well 2. The most accurate methods (Duns-Ros and Griffith-Wallis) were then programmed for machine computation and further tested against 148 well conditions.*

Neither method proved accurate over the entire range of conditions used. Although the Griffith-Wallis method was reliable in the lower flow-rate range of slug flow, it was not accurate in the higher range. The Duns-Ros method exhibited the same behavior except that it was also inaccurate for the high-viscosity oils in the low flow-rate range. The Griffith-Wallis method appeared to provide the better foundation for an improved general solution although its predicted values were in greater error (21.9 percent) than Duns and Ros (2.4 percent). The heart of this method, prediction of slip velocity, is derived from physical observation. However, since friction drop was

*The data in Table 1 are from 22 Venezuelan heavy-oil wells. In addition to the data presented in Table 1, the data used are from the publications of Poettmann and Carpenter,[1] Baxendell and Thomas,[3] Fancher and Brown,[6] and Hagedorn and Brown.[9] These represent 126 additional pieces of data.

TABLE 1—PHYSICAL CONDITIONS AND FLOW RATES OF HEAVY-OIL WELLS STUDIED

Well No.	Oil Rate (B/D)	GOR (scf/bbl)	Water Cut (%)	Oil Gravity (°API)	Measured Depth (ft)	Wellhead Pressure (psig)	Flow String Diameter (in.)	Measured Δp (psi)
1	320	4020	30	10.3	4360	250	8.76	810
2	175	6450	17	9.5	4360	300	8.76	925
3	1065	765	—	15.1	3825	550	2.992	650
4	1300	252	—	14.6	3940	150	"	850
5	3166	1430	—	14.4	3800	700	"	550
6	1965	232	—	14.4	3720	300	"	900
7	1165	957	—	15.6	4240	700	"	850
8	1965	1500	—	13.5	4570	850	"	650
9	2700	267	—	15.6	4175	300	"	1200
10	855	185	—	12.9	4355	250	"	1450
11	2320	1565	—	13.6	4670	910	"	740
12	2480	858	—	18.6	4575	650	"	900
13	1040	472	—	18.6	4400	400	"	950
14	1490	341	—	13.0	4065	500	"	1050
15	1310	335	—	13.6	3705	500	"	950
16	1350	185	—	12.9	4160	150	"	1350
17	788	222	—	16.0	4210	350	"	1400
18	1905	962	—	14.1	4487	580	"	720
19	967	193	—	13.3	4766	250	"	1300
20	1040	385	—	12.5	4505	250	"	1100
21	1585	865	—	12.9	4692	400	"	750
22	1850	575	—	18.7	3924	700	"	800

negligible in the work, the method for predicting friction losses is an approximation and therefore open to improvement. On the other hand, the Duns and Ros work in this range (which they termed plug flow) is presented as a complex set of interrelated parameters and equations, and is therefore difficult to relate to what physically occurs inside the pipe.

The Griffith-Wallis work was extended to include the high-velocity flow range. In modifying the method, a parameter was developed to account for (1) the liquid distribution among the liquid slug, the liquid film and entrained liquid in the gas bubble and (2) the liquid holdup at the higher flow velocities. This parameter served to better approximate wall friction losses and flowing density, and was principally correlated from the earlier published data of Hagedorn and Brown.[9] The data from Table 1 were also used to determine the effects of pipe diameter on the parameter. The details of the parameter evaluation are given in Appendix C and a brief description of the modified Griffith-Wallis method is outlined in Appendix A.

The results of the study, summarized in Table 2, are presented as the deviations between predicted and measured values for the modified Griffith-Wallis, the Duns-Ros and the then recently published Hagedorn-Brown[10] methods. (The Hagedorn-Brown method was included because of the excellent accuracies reported and the broad data range presented.) Plots of the individual predicted and measured values for the three methods are shown in Figs. 3 through 5. When the three methods are compared against the various grouped data sources (Table 2), only the modified Griffith-Wallis method is sufficiently accurate (average error) and precise (standard deviation) over the entire range of conditions. None of the 148 well conditions studied were in mist flow or wholly in (annular-slug) transition. The breakdown of wells by flow regimes includes seven partly in slug and transition, 26 partly in slug and bubble, four completely in bubble and 111 completely in slug flow.

CONCLUSIONS

For general engineering work, the modified Griffith-Wallis method will predict pressure drops with sufficient accuracy and precision over a wide range of well conditions. I recommend its use. However, the method should be used with discretion for those well conditions which were not sufficiently evaluated (e.g., flow in the casing annulus and in the mist-flow regime). The method's precision might be further improved if the liquid phase distribution could be more rigorously analyzed.

This method is accurate over a broader range than previous correlations. For a prediction method to be general, it must be expressed in terms of flow regime and liquid distribution. The other methods, which were not de-

TABLE 2—SUMMARY OF DEVIATIONS BETWEEN MEASURED AND PREDICTED PRESSURE DROPS

	Prediction Method		
	This Method	Duns and Ros	Hagedorn and Brown
Over-all Results			
(148 Well conditions)			
Avg. error, percent	− 0.8	+ 2.4	+ 0.7
Std. deviation, percent	10.8	27.0	24.2
Results from Grouped Data Sources			
Table 1 — Heavy-Oil Wells (22 Wells, low to medium velocities, 10 to 20° API oils)			
Avg. error, percent	− 1.2	+22.7	+16.4
Std. deviation, percent	10.4	18.7	41.4
Baxendell-Thomas[3] (1 Well, 25 rates mostly high velocities, 34° API oil)			
Avg. error, percent	− 2.1	+ 2.3	+ 8.7
Std. deviation, percent	11.1	20.0	12.7
Fancher-Brown[6] (1 Well, 20 rates medium to high velocities, 95 percent water cut)			
Avg. error, percent	+ 0.3	+ 1.7	+ 5.4
Std. deviation, percent	11.8	32.1	10.8
Hagedorn-Brown[9] (1 Well, medium to high velocities, 16 water runs, 16 oil runs of 10 to 100 cp oil)			
Avg. error, percent	+ 0.1	−16.9	+ 1.2
Std. deviation, percent	8.2	36.6	10.3
Poettmann-Carpenter[1] (49 Wells, low to medium velocities, 15 wells high water cut, rest 36 to 54° API oils)			
Avg. error, percent	− 1.0	+ 5.8	−13.0
Std. deviation, percent	12.0	12.4	22.2

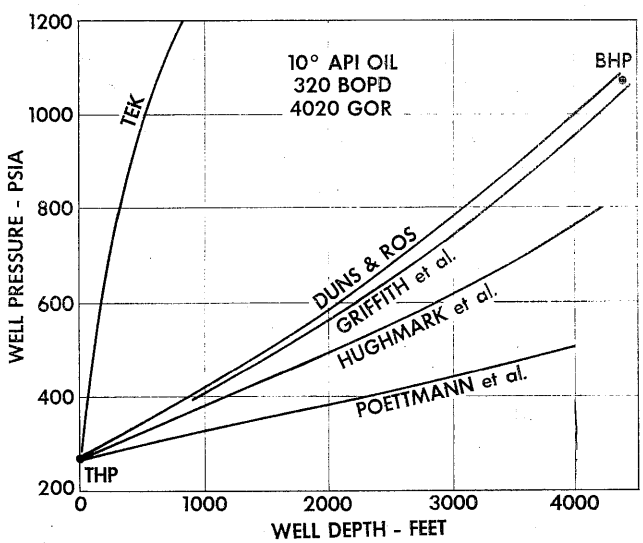

FIG. 2—COMPARISON OF PRESSURE PROFILES CALCULATED BY VARIOUS METHODS FOR WELL 1 (TABLE 1).

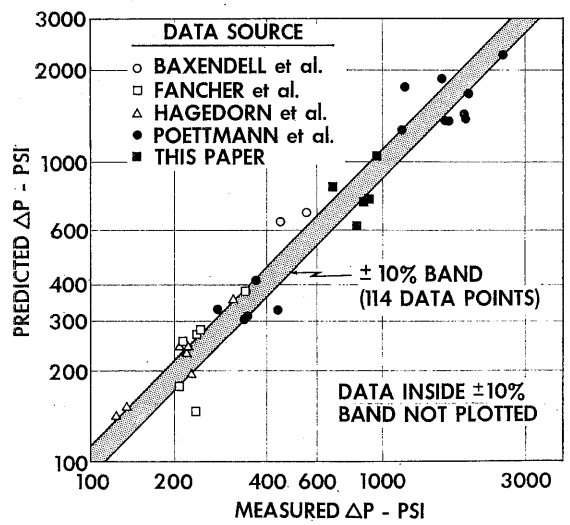

FIG. 3—THIS WORK (MODIFIED GRIFFITH AND WALLIS PREDICTION).

veloped in this manner, are only useful in the range of conditions from which they were developed.

NOMENCLATURE

A_p = flow area of pipe, sq ft
B_o = oil formation volume factor, bbl/STB
C_1, C_2 = parameters used to calculate bubble rise velocities from Eq. C-5, dimensionless, to be evaluated from Figs. 8 and 9
d_h = hydraulic pipe diameter ($4 \times A_p$/wetted perimeter), ft
D = depth from wellhead, ft
ΔD = increment of depth, ft
f = Moody friction factor, dimensionless, to be evaluated from Fig. 6
F_g = flowing gas fraction, dimensionless
g = acceleration of gravity, ft/sec^2
g_c = gravitational constant, ft-lb(mass)/lb(force)-sec^2
$(L)_B$ = bubble-slug boundary, dimensionless
$(L)_M$ = transition-mist boundary, dimensionless
$(L)_S$ = slug-transition boundary, dimensionless
N_b = 1,488 $v_b d_h \rho_L/\mu_L$, bubble Reynolds number, dimensionless
N_{Re} = 1,488 $v\ D_h\ \rho/\mu$, Reynolds number, dimensionless
p = pressure, psia
Δp = pressure drop, psi
$\overline{p}$ = average pressure, psia
p_{pc} = pseudo-critical pressure, psia
p_r = reduced pressure, dimensionless
P = pressure, lb/sq ft
q = volumetric flow rate, cu ft/sec
q_o = oil rate, B/D
R = produced GOR, scf/STB
R_s = solution gas, scf/STB
T_{pc} = pseudo-critical temperature, °R
T_r = reduced temperature, dimensionless
$\overline{T}$ = average temperature, °F
v = fluid velocity, ft/sec
v_b = bubble rise velocity (velocity of rising gas bubble relative to preceding liquid slug), ft/sec
v_{bz} = base bubble rise velocity for Eq. C-9, ft/sec
v_s = slip velocity (difference between average gas and liquid velocities), ft/sec
v_{gD} = $q_g\ (\sqrt[4]{\rho_L/g\sigma})/A_p$, dimensionless gas velocity
z = gas compressibility factor, dimensionless
γ = fluid specific gravity, dimensionless
Γ = liquid distribution coefficient, to be evaluated from Eqs. C-11 through C-16, dimensionless
μ = viscosity, cp
ξ/D = Moody pipe relative roughness factor (Fig. 7) and Duns-Ros mist flow factor (Eqs. C-21 and C-22), dimensionless
ρ = density, lb/cu ft
$\overline{\rho}$ = average flowing density, lb/cu ft
τ_f = friction-loss gradient, lb/sq ft/ft
σ = surface tension, lb/sec^2

SUBSCRIPTS

g = gas
L = liquid
o = oil
t = total

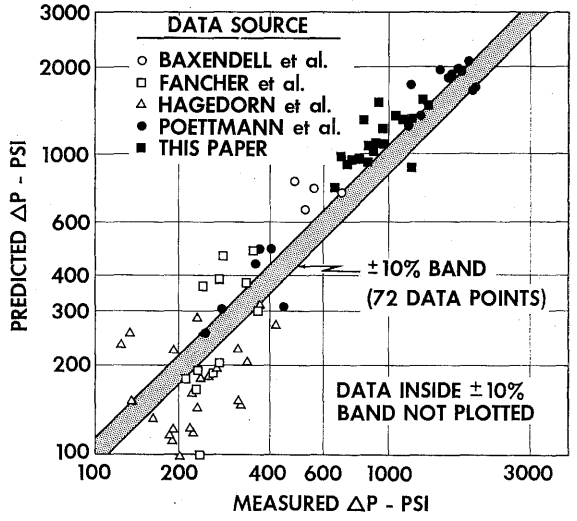

FIG. 4—DUNS AND ROS PREDICTION.[2]

ACKNOWLEDGMENT

The author wishes to thank the Creole Petroleum Corp. for supplying data in Table 1 from 22 Venezuelan heavy-oil wells.

REFERENCES

1. Poettmann, F. H. and Carpenter, P. G.: "The Multiphase Flow of Gas, Oil, and Water Through Vertical Flow Strings", *Drill. and Prod. Prac.*, API (1952) 257.
2. Duns, H., Jr., and Ros, N. C. J.: "Vertical Flow of Gas and Liquid Mixtures from Boreholes", *Proc.*, Sixth World Pet. Congress, Frankfort (June 19-26, 1963) Section II, Paper 22-PD6.
3. Baxendell, P. B. and Thomas, R.: "The Calculation of Pressure Gradients in High-Rate Flowing Wells", *J. Pet. Tech.* (Oct., 1961) 1023-1028.
4. Tek, M. R.: "Multiphase Flow of Water, Oil, and Natural Gas Through Vertical Flow Strings", *J. Pet. Tech.* (Oct., 1961) 1029-1036.
5. Yocum, B. T.: "Two-Phase Flow in Well Flowlines", *Pet. Eng.* (Nov., 1959) B-40.
6. Fancher, G. H., Jr., and Brown, K. E.: "Prediction of Pressure Gradients for Multiphase Flow in Tubing", *Soc. Pet. Eng. J.* (March, 1963) 59-69.
7. Baker, W. J. and Keep, K. R.: "The Flow of Oil and Gas Mixtures in Wells and Pipelines: Some Useful Correlations", *J. Inst. of Pet.* (May, 1961) **47**, No. 449, 162-169.
8. Hughmark, G. A. and Pressburg, B. S.: "Hold-Up and Pressure Drop with Gas-Liquid Flow in a Vertical Pipe", *AIChE J.* (Dec., 1961) **7**, No. 4, 677-682.
9. Hagedorn, A. R. and Brown, K. E.: "The Effect of Liquid Vis-

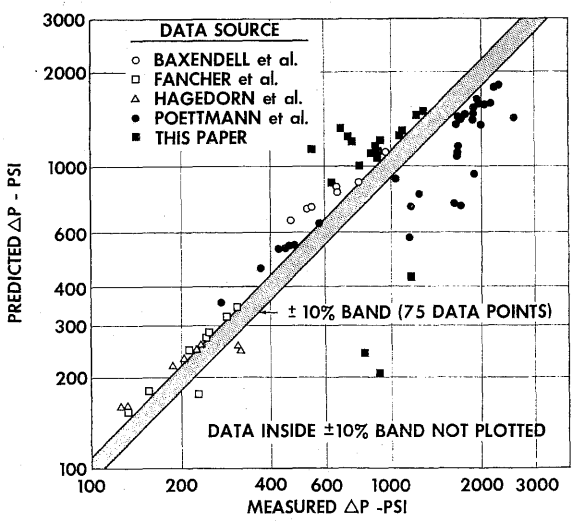

FIG. 5—HAGEDORN AND BROWN PREDICTION.[10]

cosity on Two-Phase Flow", *J. Pet. Tech.* (Feb., 1964) 203-210.

10. Hagedorn, A. R. and Brown, K. E.: "Experimental Study of Pressure Gradients Occurring During Continuous Two-Phase Flow in Small Diameter Vertical Conduits", *J. Pet. Tech.* (April, 1965) 475-484.

11. Griffith, P. and Wallis, G. B.: "Two-Phase Slug Flow", *J. Heat Transfer; Trans.*, ASME (Aug., 1961) 307-320.

12. Griffith, P.: "Two-Phase Flow in Pipes", Special Summer Program, Massachusetts Institute of Technology, Cambridge, Mass. (1962).

13. Nicklin, D. J., Wilkes, J. O. and Davidson, J. F.: "Two-Phase Flow in Vertical Tubes", *Trans.*, AIChE (1962) **40**, 61-68.

14. Stanley, D. W.: "Wall Shear Stress in Two-Phase Slug Flow", MS Thesis, Massachusetts Institute of Technology, Cambridge (June, 1962).

15. Moody, L. F.: "Friction Factors in Pipe Flow", *Trans.*, ASME (1944) **66**, 671-684.

16. Frick, T. C.: *Petroleum Production Handbook—Vol. II, Reservoir Engineering*, McGraw-Hill, New York (1962).

APPENDIX A

DESCRIPTION OF MODIFIED GRIFFITH AND WALLIS METHOD*

The fluid pressure drop in a vertical pipe is the sum effect of the energy lost by friction, the change in potential energy and the change in kinetic energy. This energy balance, which is basic to all pressure-drop calculations, can be generally written as

$$-dP = \tau_f dD + (g\rho/g_c)dD + (\rho v/g_c)dv \quad , \quad . \quad . \quad \text{(A-1)}$$

where P = pressure, lb/sq ft,
τ_f = friction-loss gradient, lb/sq ft/ft,
D = depth, ft,
g = acceleration of gravity, ft/sec^2,
g_c = gravitational consant, ft-lb(mass)/lb(force)-sec^2,
ρ = fluid density, lb/cu ft,
v = fluid velocity, ft/sec.

The procedure was credited to Griffith and Wallis because slug flow occurred in 95 percent of the cases studied. Although the mist-flow regime could not be evaluated, the Duns-Ros method was used because it appeared to be more accurate and logical than the Martinelli method recommended by Griffith. In two-phase flow, both τ_f and ρ are influenced by the flow regime type, and all three terms are functions of temperature and pressure. Therefore, to use Eq. A-1, (1) the flow string must be incremented so the fluid properties do not change markedly within any of the increments, (2) the flow regime type and corresponding variables of $\bar{\rho}$ and τ_f must be determined for each increment and (3) each increment must be evaluated by an iterative procedure.

The kinetic energy term is significant only in the mist-flow regime.[2] In mist flow $v_L << v_g$, the kinetic energy term may be expressed[1] more simply (using the gas law).

$$(\rho v/g_c)dv = -\frac{w_t q_g}{g_c A_p^2 P} dP \quad , \quad . \quad . \quad . \quad . \quad . \quad . \quad . \quad \text{(A-2)}$$

where A_p = pipe area, sq ft,

w_t = total mass flow rate, lb/sec,**

q_g = gas volumetric flow rate, cu ft/sec.**

With the above conditions and Eq. A-2, Eq. A-1 may then be expressed in a more convenient form.***

$$\Delta p_k = \left[\frac{1}{144} \frac{\bar{\rho} + \tau_f}{1 - w_t q_g / 4{,}637 A_p^2 \bar{p}} \right]_k \Delta D_k \quad , \quad \text{(A-3)}$$

where for average temperature-pressure conditions at increment k,

$\bar{\rho}$ = average fluid density, lb/cu ft,
Δp = pressure drop, psi,
$\bar{p}$ = average pressure, psia.

Since temperature is related to depth, Eq. A-3 may be incremented by either fixing ΔD and solving for Δp, or vice versa. However, since pressure usually has a greater influence on the average fluid properties than temperature, Δp should be fixed because the change in average fluid properties would then be more gradual in going from one increment to another. The value of Δp should be around 10 percent of the absolute pressure, which is known for one point in the increment, but should not be greater than 100 psi for that increment.

Pressure drops can be calculated, using Eq. A-3 in the following manner.

1. Pick a point in the flow string (e.g., wellhead or bottom-hole) where the flow rates, fluid properties, temperature and pressure are known.

2. Estimate the temperature gradient of the well.

3. Fix the Δp at about 10 percent of the measured or previously calculated pressure, which may be at either the top or bottom of the increment. Find average pressure of increment.

4. Assume a depth increment ΔD and find average depth of increment.

5. From the temperature gradient, determine average temperature of increment.

6. Correct fluid properties for temperature and pressure.

7. Determine the type of flow regime from Appendix B.

8. Based on Step 7, determine the average density ($\bar{\rho}$) and the friction loss gradient (τ_f) from Appendix C.

9. Calculate ΔD from Eq. A-3.

10. Iterate, if necessary, starting with Step 4 until assumed ΔD equals calculated ΔD.

11. Determine values of p and D for that increment.

12. Repeat procedure from Step 3 until the sum of the ΔD's equals the total length of the flow string.

A detailed example of the above calculated procedure is given in Appendix D.

APPENDIX B

DETERMINATION OF FLOW REGIME

Griffith and Wallis have defined the boundary between bubble and slug flow,[11] and Duns and Ros have defined the boundaries for the remaining three regimes.[2] The flow regime may be determined by testing whether the variables q_g/q_t or v_{gD}, or both, fall within the limits prescribed.

*This method is a composite of the following:

Method	Flow Regime
Griffith[12]	Bubble
Griffith and Wallis[11]	Slug (density term)
This work	Slug (friction gradient term)
Duns and Ros[2]	Transition
Duns and Ros[2]	Annular-mist

**All volumetric (q) and mass (w) flow rates are those of the produced fluids that are corrected for temperature, pressure and gas solubility.

***$\triangle Z$ is taken as positive downward. The pressure should be made discontinuous with depth should the denominator approach zero, or become negative, to estabish the shock front that characterizes sonic velocities.

Limits	Flow Regime
$q_g/q_t < (L)_B$	Bubble
$q_g/q_t > (L)_B$, $v_{gD} < (L)_S$	Slug
$(L)_M > \tilde{v}_g > (L)_S$	Transition
$v_{gD} > (L)_M$	Mist

The above variables are defined as

$$v_{gD} = q_g(\sqrt[4]{\rho_L/g\,\sigma})/A_p \quad . \quad . \quad . \quad . \quad . \quad . \quad . \quad . \quad . \quad \text{(B-1)}$$

$$(L)_B = 1.071 - (0.2218\, v_t^2/d_h, \text{ with the limit } (L) \geq 0.13 \quad . \quad . \quad . \quad . \quad . \quad . \quad . \quad . \quad . \quad \text{(B-2)}$$

$$(L)_S = 50 + 36\, v_{gD}\, q_L/q_g \quad . \quad . \quad . \quad . \quad . \quad . \quad . \quad . \quad \text{(B-3)}$$

$$(L)_M = 75 + 84\,(v_g\, q_L/q_g)^{0.75} \quad , \quad . \quad . \quad . \quad . \quad . \quad . \quad . \quad \text{(B-4)}$$

where v_{gD} = dimensionless gas velocity,

v_t = total fluid velocity (q_t/A_p), ft/sec,

ρ_L = liquid density, lb/cu ft,

σ = liquid surface tension, lb/sec^2.

APPENDIX C

EVALUATION OF AVERAGE DENSITY AND FRICTION LOSS GRADIENT

In the first four sections of this Appendix, the variables $\overline{\rho}$ and τ_f are defined for bubble flow, slug flow, transition and mist flow. The second section, while the most complex, is also the most important since slug flow had been encountered in over 95 percent of the gas-lift or flowing wells studied. The last section of this Appendix describes how τ_f was developed for the slug flow regime.

BUBBLE FLOW (REF. 12)

The void fraction of gas (F_g) in bubble flow can be expressed as

$$F_g = \frac{1}{2}\left[1 + \frac{q_t}{v_s A_p} - \sqrt{(1 + q_t/v_s A_p)^2 - \frac{4q_g}{v_s A_p}}\right], \quad . \quad . \quad . \quad . \quad . \quad . \quad . \quad . \quad . \quad \text{(C-1)}$$

where v_s = slip velocity in ft/sec. Griffith suggested that a good approximation of an average v_s is 0.8 ft/sec.* Thus, with Eq. C-1, the average flowing density can be computed as

$$\overline{\rho} = (1 - F_g)\,\rho_L + F_g\rho_g \quad . \quad . \quad . \quad . \quad . \quad . \quad . \quad . \quad \text{(C-2)}$$

The friction gradient is

$$\tau_f = f_{\rho_L} v_L^2/2g_c d_h \quad , \quad . \quad . \quad . \quad . \quad . \quad . \quad . \quad . \quad . \quad \text{(C-3)}$$

where

$$v_L = q_L/[A_p\,(1 - F_g)]\,.$$

The friction factor f is obtained from Fig. 6 by using a Moody relative-roughness factor obtained from Fig. 7. The Reynolds number is calculated as $N_{Re} = 1{,}488\ \rho_L d_h v_L/\mu_L$; where d_h = hydraulic pipe diameter, ft, and μ_L = liquid viscosity, cp.

SLUG FLOW (REF. 11)

The average density term is

$$\overline{\rho} = \frac{w_t + \rho_L v_b A_p}{q_t + v_b A_p} + \Gamma\,\rho_L \quad , \quad . \quad . \quad . \quad . \quad . \quad . \quad . \quad \text{(C-4)}$$

*Although the method is simple, it is reasonably precise. For the four wells that were wholly in bubble flow, the standard deviation was 5.1 percent, whereas the deviation was 9.8 percent for those wells partly in bubble and slug.

where Γ is a coefficient correlated from oilfield data. Griffith and Wallis correlated the bubble rise velocity v_b by the relationship

$$v_b = C_1 C_2 \sqrt{g\,d_h} \quad , \quad . \quad . \quad . \quad . \quad . \quad . \quad . \quad . \quad . \quad \text{(C-5)}$$

where C_1 is expressed in Fig. 8 as a function of bubble Reynolds number ($N_b = 1{,}488\ v_b d_h \rho_L/\mu_L$), and C_2 is expressed in Fig. 9 as a function of both N_b and liquid Reynolds number.

$$N_{Re} = 1{,}488\ \rho_L d_h v_t/\mu_L \quad , \quad . \quad . \quad . \quad . \quad . \quad . \quad . \quad . \quad \text{(C-6)}$$

where v_t equals total velocity of liquid and gas (q_t/A_p), ft/sec.

Fig. 9 was extrapolated** so that v_b could be evaluated at the higher Reynolds numbers. When C_2 cannot be read

**The parallel work of Nicklen, Wilkes and Davidson[13] provided the basis for the extrapolation. It showed that bubble rise velocity was independent of N_b in the Reynolds number range of 9×10^3 to 1×10^5. The correlation of bubble rise velocity was found comparable to Eq. C-5 when N_b was around 8×10^3. The results were incorporated into the above extrapolation.

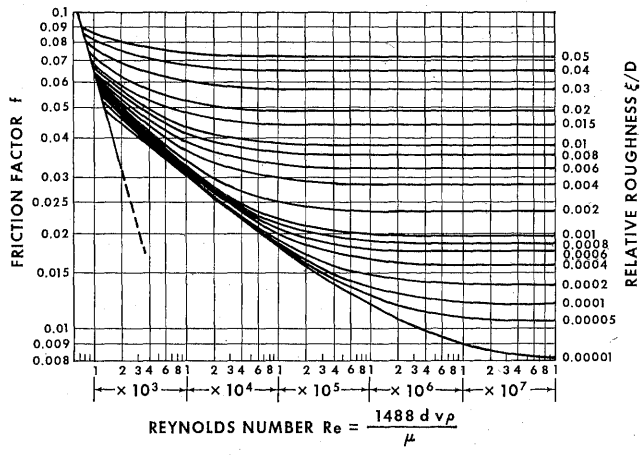

FIG. 6—MOODY FRICTION FACTOR.[15]

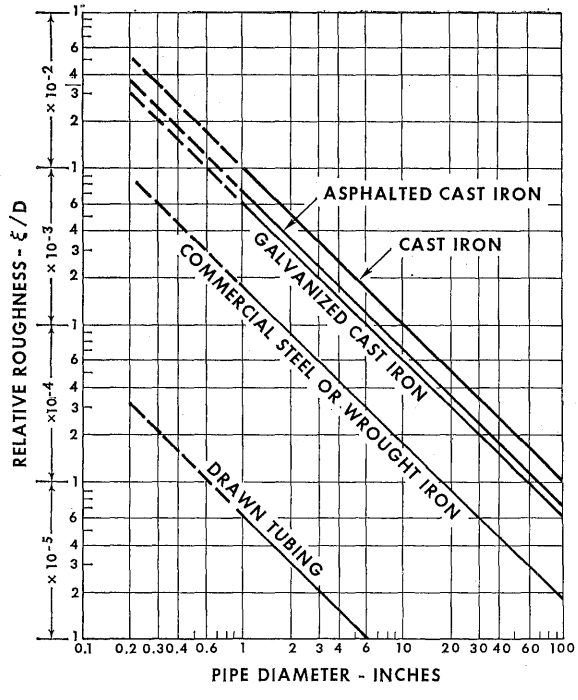

FIG. 7—EFFECT OF PIPE DIAMETER AND MATERIAL ON RELATIVE ROUGHNESS.[15]

from Fig. 9, the extrapolated values of v_b may be calculated from the following set of equations.

When $N_b \leq 3{,}000$,

$$v_b = (0.546 + 8.74 \times 10^{-6} N_{Re}) \sqrt{gd_h} \quad . \quad . \quad . \quad \text{(C-7)}$$

When $N_b \geq 8{,}000$,

$$v_b = (0.35 + 8.74 \times 10^{-6} N_{Re}) \sqrt{gd_h} \quad . \quad . \quad . \quad \text{(C-8)}$$

When $3{,}000 < N_b < 8{,}000$,

$$v_{bi} = (0.251 + 8.74 \times 10^{-6} N_{Re}) \sqrt{gd_h},$$

$$v_b = \frac{1}{2} v_{bi} + \sqrt{v_{bi}^2 + \frac{13.59\,\mu_L}{\rho_L \sqrt{d_h}}} \quad . \quad . \quad . \quad . \quad . \quad \text{(C-9)}$$

The wall friction-loss term, which has been independently derived, is expressed as

$$\tau_f = \frac{f\rho_L v_t^2}{2g_c d_h}\left[\frac{q_L + v_b A_p}{q_t + v_b A_p} + \Gamma\right] \quad . \quad . \quad . \quad . \quad . \quad \text{(C-10)}$$

The friction factor is obtained from Fig. 6 and is a function of the Reynolds number given by Eq. C-6 and the ξ/D obtained from Fig. 7. The liquid distribution coefficient Γ may be determined by the equation which meets the following conditions.

Continuous Liquid Phase	v_t	Use Equation
Water	<10	C-11
Water	>10	C-12
Oil	<10	C-13
Oil	>10	C-14

$$\Gamma = [(0.013 \log \mu_L)/d_h^{1.38}] - 0.681 + 0.232 \log v_t - 0.428 \log d_h \quad . \quad . \quad . \quad . \quad . \quad . \quad . \quad \text{(C-11)}$$

$$\Gamma = [(0.045 \log \mu_L)/d_h^{0.799}] - 0.709 - 0.162 \log v_t - 0.888 \log d_h \quad . \quad . \quad . \quad . \quad . \quad . \quad . \quad \text{(C-12)}$$

$$\Gamma = [0.0127 \log (\mu_L + 1)/d_h^{1.415}] - 0.284 + 0.167 \log v_t + 0.113 \log d_h \quad . \quad . \quad . \quad \text{(C-13)}$$

$$\Gamma = [0.0274 \log (\mu_L + 1)/d_h^{1.371}] + 0.161 + 0.569 \log d_h - \log v_t \{[0.01 \log (\mu_L + 1)/d_h^{1.571}] + 0.397 + 0.63 \log d_h\} \quad , \quad . \quad . \quad . \quad . \quad . \quad \text{(C-14)}$$

but is constrained by the limits

$$\Gamma \geq -0.065\, v_t \quad , \quad . \quad . \quad . \quad . \quad . \quad . \quad . \quad . \quad . \quad \text{(C-15)}$$

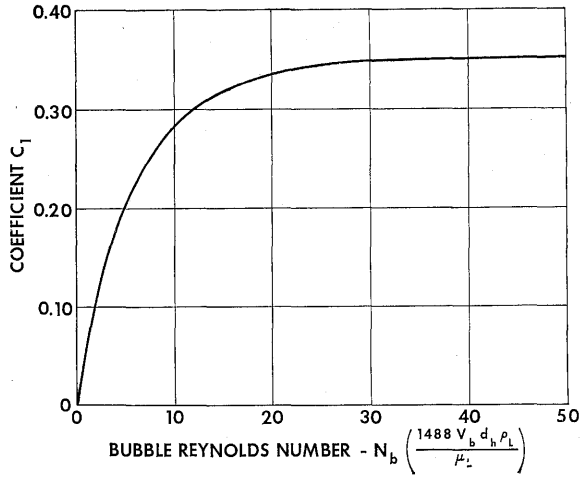

FIG. 8—GRIFFITH AND WALLIS' C_1 VS BUBBLE REYNOLDS NUMBER.

and when $v_t > 10$,

$$\Gamma \geq -\frac{v_b A_p}{q_t + v_b A_p}\left(1 - \frac{\bar{\rho}}{\rho_L}\right) \quad . \quad . \quad . \quad . \quad . \quad \text{(C-16)}$$

The above constraints eliminate pressure discontinuities between flow regimes.

TRANSITION FLOW

Duns and Ros approximated $\bar{\rho}$ and τ_f for transition flow. The method is first to calculate these terms for both slug and mist flow, and then linearly weight each term with respect to v_{gD} and the limits of the transition zone $(L)_S$ and $(L)_M$. The terms v_{gD}, $(L)_M$ and $(L)_S$ are defined in Appendix B. The average density term would be

$$\bar{\rho} = \frac{(L)_M - v_{gD}}{(L)_M - (L)_S}\left[\bar{\rho}\right]_{slug} + \frac{v_{gD} - (L)_S}{(L)_M - (L)_S}\left[\bar{\rho}\right]_{mist} \quad . \quad . \quad . \quad . \quad . \quad . \quad . \quad . \quad . \quad \text{(C-17)}$$

The friction gradient term would be weighted similarly. A more accurate friction-loss prediction is claimed if the gas volumetric flow rate for mist flow is taken as

$$q_g = A_p (L)_M (\rho_L/g\sigma)^{-1/4} \quad . \quad . \quad . \quad . \quad . \quad . \quad . \quad \text{(C-18)}$$

MIST FLOW

The average flowing density for mist flow is given in Eq. C-2. Since there is virtually no slip between the phases, F_g is

$$F_g = 1/(1 + q_L/q_g) \quad . \quad . \quad . \quad . \quad . \quad . \quad . \quad . \quad . \quad \text{(C-19)}$$

Duns and Ros express the friction-loss gradient as

$$\tau_f = f\,\rho_g v_g^2/2g_c d_h \quad , \quad . \quad . \quad . \quad . \quad . \quad . \quad . \quad \text{(C-20)}$$

where v_g is the superficial gas velocity, and f is again obtained from Fig. 6 as a function of gas Reynolds number ($N_{Re} = 1{,}488\, p_g d_h v_g/\mu_g$) and a correlated form of the Moody relative roughness factor ξ/D that was developed by Duns and Ros. In their correlation, they limit ξ/D to being no smaller than 10^{-3} but no greater than 0.5. Between these limits, ξ/D is determined from Eq. C-21 if N_w is less than 0.005 and from Eq. C-22 if N_w is greater than 0.005.

$$\xi/D = 34\,\sigma/(\rho_g v_g^2 d_h) \quad . \quad . \quad . \quad . \quad . \quad . \quad . \quad . \quad . \quad \text{(C-21)}$$

$$\xi/D = 174.8\,\sigma\,(N_w)^{0.302}/(\rho_g v_g^2 d_h) \quad , \quad . \quad . \quad . \quad . \quad \text{(C-22)}$$

where $N_w = 4.52 \times 10^{-7} (v_g \mu_L/\sigma)^2\, \rho_g/\rho_L$.

DEVELOPMENT OF τ_f FOR SLUG FLOW

A new method was developed to correlate the friction-loss gradient for slug flow because neither the Griffith and Wallis method, nor the Stanley[14] method (an outgrowth of the Griffith-Wallis work) proved accurate for the well conditions studied. (The Griffith-Wallis data were taken

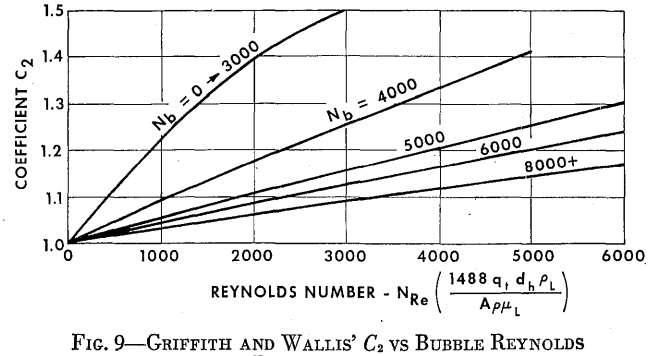

FIG. 9—GRIFFITH AND WALLIS' C_2 VS BUBBLE REYNOLDS AND REYNOLDS NUMBERS.

from low-flow velocity tests in which friction losses were minor and liquid entrainment was negligible.) This new method accounted for the complex nature of friction loss in slug flow by the introduction of a correlated liquid distribution function Γ (Eq. C-10) which implicitly accounts for the following physical phenomena.

1. Liquid is distributed in three places: the slug, the film around the gas bubble and in the gas bubble as entrained droplets. A change in this distribution will change the net friction losses.

2. The friction loss has essentially two contributions, one from the liquid slug and the other from the liquid film.

3. The bubble rise velocity approaches zero as mist flow is approached.

Values of the liquid distribution coefficient were calculated from the data of Hagedorn and Brown[9] by using Eq. A-3 of Appendix A and Eqs. C-4 through C-10 of Appendix C. (These data were selected because they covered a wide range of conditions for each of the four liquids used.) These values correlate with total fluid velocity and liquid viscosity. Fig. 10 shows the results where the fluid is water, and Fig. 11 shows the results where the fluids are oil. Coefficients were also calculated for the heavy-oil wells shown in Table 1, but these values were small and scattered because τ_f was small in comparison to $\overline{\rho}$. Nevertheless, the results were sufficiently grouped to show that pipe diameter (d_h) is another independent variable.

Neither the reversal in slopes nor the data scatter as seen in Figs. 10 and 11 can be resolved without additional experimental work. It is probable, however, that the slope reversal may be due to liquid entrained in the gas phase

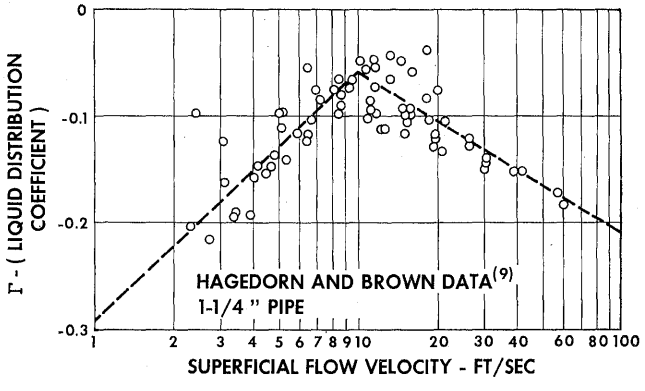

FIG. 10—EFFECT OF VELOCITY ON WATER DISTRIBUTION COEFFICIENT.

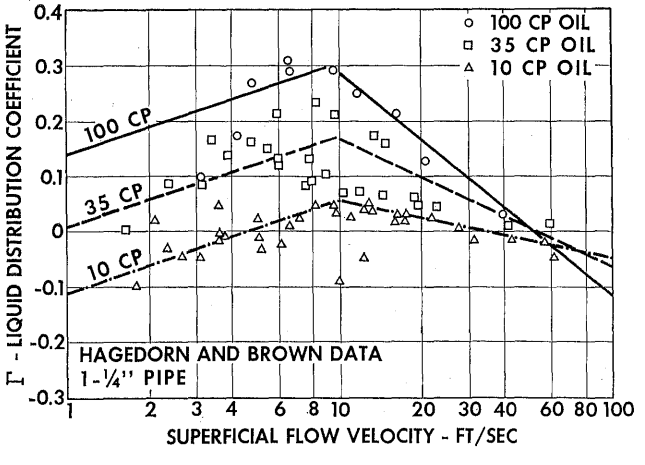

FIG. 11—OIL DISTRIBUTION COEFFICIENT AFFECTED BY BOTH VELOCITY AND VISCOSITY.

TABLE 3 — FLOW RATES AND PHYSICAL CONDITIONS OF HEAVY-OIL WELL 22

Oil Rate (q_o)	1,850 STB/D	Oil Specific Gravity (γ_o)	0.942
Produced GOR (R)	575 scf/ STB	Gas Specific Gravity (γ_g)	0.75
Total depth (D)	3,890 ft	Wellhead Pressure	670 psia
Tubing diameter (d_h)	0.249 ft	Tubing Area A_p	0.0488 sq ft
Temperatures:		Dead Oil Viscosity:	
Wellhead	126F	at 100F	89 cp
Reservoir	150F	at 210F	8.8 cp

and that the data scatter may be attributable to such additional parameters as liquid velocity, GOR and interfacial tension.

APPENDIX D

EXAMPLE OF TWO-PHASE PRESSURE DROP CALCULATION

An example calculation of the modified Griffith-Wallis method is presented to illustrate the details of the procedure outlined in Appendix A. In this example we will predict the pressure drop for heavy-oil Well 22 (Table 1). The input well data required for the calculation are given in Table 3. In addition, we will need the following correlations* that correct fluid properties for pressure and temperature:

Gas pseudo-critical properties (Katz *et al.*) T_{pc}, p_{pc}.

Gas compressibility (Brown *et al.*) z.

Live oil viscosity (Chew and Connally) μ.

Oil formation volume factor (Standing) B_o.

Solution gas (Lasater) R_s.

For calculational convenience, the temperature-viscosity-depth data contained in Table 3 should be plotted. The temperature-depth plot is shown in Fig. 12, and log viscosity-log temperature plot is shown in Fig. 13.

The detailed procedure for the calculation of the pressure drop for the first increment ($k = 1$) is as follows.

1. Based on the 670-psia wellhead pressure, fix Δp at 100 psi. Assume ΔD to be 540 ft. The average pressure ($\overline{p}$) and depth ($\overline{D}$) of increment k is then:

$$\overline{p}_k = p_{k-1} + \frac{\Delta p_k}{2} = 670 + \frac{100}{2} = 720 \text{ psia}$$

$$\overline{D}_k = D_{k-1} \frac{\Delta D_k}{2} = 0 + \frac{540}{2} = 270 \text{ ft.}$$

The average temperature ($\overline{T}$), read from Fig. 12 is 127.5F.

*These are conveniently found in Frick's *Petroleum Production Handbook, Vol. II* (Ref. 16).

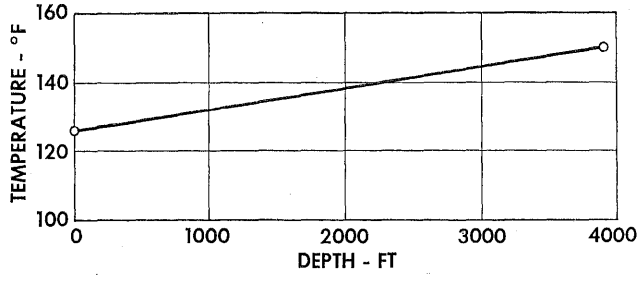

FIG. 12—TEMPERATURE VS DEPTH — WELL 22.

2. With the condition determined in Step 1, the fluid properties are corrected for temperature and pressure.

From Frick[16] the following values are obtained.

R_s = 115 scf/bbl (page 19-9).*

B_o = 1.073 bbl/STB (page 19-25).

p_{pc} = 665 psia (page 17-6).

T_{pc} = 415R (page 17-6).

μ = 18 cp** (page 19-40).

The gas compressibility c is determined as

$$T_r = \frac{\overline{T} + 460}{T_{pc}} = \frac{587.5}{415} = 1.42$$

$$p_r = \frac{\overline{p}}{P_{pc}} = \frac{720}{665} = 1.08,$$

and from Frick (page 17-15),

$z = 0.875$.

The corrected volumetric flow rates are

$$q_L = 6.49 \times 10^{-5} q_o B_o = 6.49 \times 10^{-5} (1{,}850)(1.073)$$
$$= 0.129 \text{ cu ft/sec}$$

$$q_g = 3.27 \times 10^{-7} z\, q_o (R - R_s) \frac{(\overline{T} + 460)}{\overline{p}}$$
$$= 3.27 \times 10^{-7} (0.875)(1{,}850)(575 - 115)(587.5)/720$$
$$= 0.199 \text{ cu ft/sec}$$

$$q_t = 0.128 + 0.199 = 0.328 \text{ cu ft/sec.}$$

The corrected mass flow rates are

$$w_L = q_o (4.05 \times 10^{-3} \gamma_o + 8.85 \times 10^{-7} \gamma_g R_s)$$
$$= 1{,}850 [4.05 \times 10^{-3} (0.942) + 8.85 \times 10^{-7} (0.75)(115)]$$
$$= 7.20 \text{ lb/sec}$$

$$w_g = 8.85 \times 10^{-7} q_o \gamma_g (R - R_s)$$
$$= 8.85 \times 10^{-7} (1{,}850)(0.75)(575 - 115)$$
$$= 0.565 \text{ lb/sec}$$

$$w_t = 7.20 + 0.57 = 7.77 \text{ lb/sec.}$$

*Parentheses indicate the page number in Frick's book[16], where the various correlations are found.

**Live oil viscosity. Dead oil viscosity, a parameter in the correlation, is read from Fig. 13.

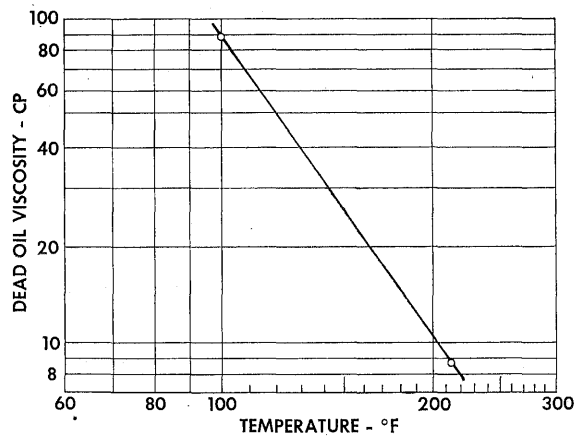

FIG. 13—DEAD OIL VISCOSITY VS TEMPERATURE — WELL 22.

The corrected densities are

$$\rho_L = w_L/q_L = 7.20/0.129 = 55.8 \text{ lb/cu ft}$$

$$\rho_g = w_g q_g = 0.565/0.199 = 2.84 \text{ lb/cu ft.}$$

3. The variables described in Appendix B are calculated and then are tested against the boundary limits to determine the flow regime.

Test Variables:

$$v_t = q_t/A_p = 0.328/0.0488 = 6.72 \text{ ft/sec.}$$

$$q_g/q_t = 0.199/0.328 = 0.607.$$

$$v_{gD} = 0.199 \left[\sqrt{0.534\,(55.8)}\right]/0.0488 = 9.53 \quad \text{(B-1)}$$

Boundary Limits:

$$(L)_B = 1.071 - \frac{0.2218\,(6.72)^2}{0.249} \quad \text{(B-2)}$$

$(L)_B = -22$. Since $(L)_B$ has the limit of 0.13,

$\therefore (L)_B = 0.13$.

$$(L)_S = 50 + 36\,(9.53)\,(0.129)/0.199 = 272 \quad \text{(B-3)}$$

Because $q_g/q_t > (L)_B$ and $v_{gD} < (L)_S$, the fluids are in slug flow.

4. The equations given in the Slug Flow section of Appendix C are used to calculate $\overline{\rho}$ and τ_f.

Determine Reynolds number, bubble Reynolds number and slip velocity (v_b).

$$N_{Re} = 1{,}488\,(55.8)\,(0.249)\,(6.72)/18 = 7{,}720 \quad \text{(C-6)}$$

Since the bubble rise velocity is a nonlinear correlation, iteration is necessary. Therefore, assuming $v_b = 1.75$, bubble Reynolds number is

$$N_b = 1{,}488\,(55.8)\,(0.249)\,(1.75)/18 = 2{,}010.$$

C_2 cannot be read from Fig. 9. Thus the extrapolation equation (Eq. C-7) is used since $N_b < 3{,}000$.

$$v_b = [0.546 + 8.74 \times 10^{-6}\,(7{,}720)]\sqrt{32.2\,(0.249)}$$
$$= 1.74 \text{ ft/sec.}$$

Determine liquid distribution coefficient Γ and friction factor f. Eq. C-13 is used to evaluate Γ since $v_t < 10$:

$$\Gamma = \left[\frac{0.0127 \log (18 + 1)}{(0.249)^{1.415}}\right] - 0.284 + 0.167 \log 6.72 + 0.113 \log 0.249 = -0.097.$$

Test limiting Γ with Eq. C-15:

$$-0.097 \geq -0.065\,(6.72)$$
$$\geq -0.436;$$

therefore, $\Gamma = -0.097$.

The ξ/D value from Fig. 7 is 0.0006. With this value and the calculated N_{Re} of 7,720, a friction factor of 0.034 is read from Fig. 6.

Evaluate $\overline{\rho}$ with Eq. C-4:

$$\overline{\rho} = \frac{7.77 + 55.8\,(1.74)\,(0.0488)}{0.328 + 1.74\,(0.0488)} + (-0.097)\,(55.8) = 24.9 \text{ lb/cu ft.}$$

Evaluate τ_f with Eq. C-10:

$$\tau_f = \frac{0.034\,(55.8)\,(6.72)^2}{64.4\,(0.249)}\left[\frac{0.129 + 1.74\,(0.0488)}{0.328 + 1.74\,(0.0488)} - 0.097\right]$$
$$= 2.26 \text{ lb/sq ft/ft.}$$

5. The depth increment from Eq. A-3 is

$$\Delta D_1 = 144\left[\frac{\Delta p_1\left(1-\frac{w_t\, q_g}{4{,}637\, A_p^{\,2}\,\bar{p}}\right)}{\bar{\rho}+\tau_f}\right]_1$$

$$= 144\left[\frac{100\left(1-\frac{7.77\,(0.199)}{4{,}637\,(0.0488)^2\,(720)}\right)}{24.9+2.3}\right]_1 = 529 \text{ ft.}$$

The true value of ΔD_1 is near 529 ft. The calculation will converge very closely to this value even when the assumed ΔZ is off by ± 10 percent of the assumed value (540 ft) because, under these well conditions, the pressure gradient is primarily controlled by the relatively temperature-insensitive density head. However, under those circumstances where the friction gradient, which is temperature sensitive, is significant, iteration would be necessary should the calculated value of ΔD differ from the assumed value by +10 percent.

6. The top of the next increment is fixed at 529 ft and 770 psi, and Steps 1 through 6 are repeated for the new conditions.

7. The procedure is continued until $\Sigma\, \Delta D$ is equal to the total depth. The calculated pressure profile is compared against the measured profile in Fig. 14. ★★★

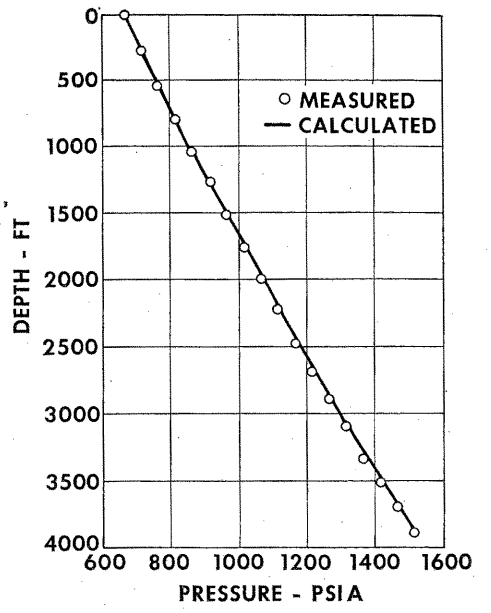

FIG. 14—CALCULATED VS MEASURED PRESSURE DROP — WELL 22.